

Functional Connectivity Brain Network Analysis through Network to Signal Transform Based on the Resistance Distance

Marisel Villafañe-Delgado and Selin Aviyente

Department of Electrical and Computer Engineering,
Michigan State University, East Lansing, MI, 48824, USA.
aviyente@egr.msu.edu

Abstract—Functional connectivity brain networks have been shown to demonstrate interesting complex network behavior such as small-worldness. Transforming networks to time series has provided an alternative way of characterizing the structure of complex networks. However, previously proposed deterministic methods are limited to unweighted graphs. In this paper, we propose to employ the resistance distance matrix of weighted graphs as the distance matrix for transforming networks to signals based on classical multidimensional scaling. We present a framework for obtaining information about the network's structure through the mapped signals and recovering the original network using properties of the resistance matrix. Finally, the proposed method is applied to characterizing functional connectivity networks constructed from electroencephalogram data.

Index Terms—Resistance distance, Complex networks, Classical multidimensional scaling, Functional brain connectivity.

I. INTRODUCTION

Advances in network analysis have provided valuable tools for a better understanding of functional connectivity in the human brain [1]. Functional connectivity has been defined as the statistical dependence among brain regions [2]. Functional connectivity has been quantified through both linear and nonlinear measures. However, these pairwise relationships cannot describe the underlying topology of the network [3]. Graph theory provides a mathematical framework that allows for further understanding of the organization of the brain. Functional connectivity networks can be constructed to model these interactions where the nodes represent brain regions or electrodes and the edges correspond to the relationships between them. Graph theoretic measures such as the clustering coefficient and characteristic path length have been used to quantify the amount of segregation and integration in these networks, respectively. However, these metrics have some limitations such as either focusing on the local organization of the network or the global topology and not directly quantifying the interaction between different subsystems of the network.

Some of the shortcomings of graph measures can be avoided by exploiting the relationships between networks and signals. Recent work in signal processing for graphs have focused on processing signals on graphs [4] and representing networks as signals [5], [6], [7]. For the latter, both deterministic and probabilistic methods based on random walk theory [7] have been proposed to convert networks into signals. Shimada [5] and Haraguchi [6] formulated a deterministic method based on classical multidimensional scaling (CMDS), allowing the transformation from complex unweighted networks to time series. Under this transformation, the nodes of the

network correspond to time indices for the time series [8]. It was shown that lattice networks transform to sinusoids and Watt-Strogatz networks transform to random signals. Recently, Hamon et. al. [9] have extended this method to the analysis of temporal networks. However, all of these approaches have focused on binary graphs, and therefore have limited applicability to weighted networks that arise in neuroscience.

In order to construct signals from both unweighted and weighted graphs, we propose to use the resistance distance of a connected graph as the distance matrix for CMDS. The resistance distance matrix of a graph was proposed in [10] in the context of chemistry. The resistance distance between two nodes corresponds to the equivalent resistance between them, considering the graph as an electric circuit [10]. Thus, the resistance distance takes into account the global structure of the graph, when compared to the shortest path distance, which reflects only information about one path. Moreover, the resistance distance can be obtained from the pseudoinverse of the combinatorial Laplacian of the graph [11] and is a valid distance matrix. Therefore, it is an alternative distance matrix for CMDS.

The following sections of this article are organized as follows. Section II presents background on graph theory, CMDS and phase synchrony for the construction of functional connectivity networks from electroencephalogram (EEG) signals. Section III presents the proposed method for transforming weighted networks into signals and reconstruction of networks from these signals. Section IV presents results comparing the proposed method to the previous method proposed by [5] for unweighted graphs. Finally, the proposed method is applied to functional connectivity networks constructed from a study of cognitive control.

II. BACKGROUND

A. Graph Theory

An undirected graph $G = (V, E)$ consists of a set of N nodes, $v_i \in V$, and a set of M edges, $e_{ij} \in E$. For unweighted graphs, the adjacency matrix $\mathbf{A} = [a_{ij}]$ is a binary matrix, where $a_{ij} = 1$ when vertices i and j are connected, and equals to zero when $i = j$ or when the vertices are not connected. For weighted graphs, the adjacency matrix \mathbf{W} has entries equal to ω_{ij} representing the weight of the edge between vertices i and j . The combinatorial Laplacian for unweighted graphs is defined as $\mathbf{L} = \Delta - \mathbf{A}$, where Δ corresponds to the degree matrix which is defined as the diagonal matrix with elements δ_i equal to the degree of node v_i . The entries of \mathbf{L} are given by

$$L_{ij} = \begin{cases} \delta_i, & i = j, \\ -1, & (i, j) \in E, \\ 0, & \text{otherwise,} \end{cases} \quad (1)$$

where δ_i is the degree of vertex v_i . Similarly, for weighted graphs the combinatorial Laplacian can be defined as $\mathbf{L}^W = \Delta^W - \mathbf{W}$, where Δ^W is a weighted degree matrix whose entries are given by $\Delta_{ii}^W = \sum_{j=1, j \neq i}^N \omega_{ij}$, where ω_{ij} corresponds to the weight between nodes i and j .

B. Classical Multidimensional Scaling

The objective of CMDS is to find a low-dimensional representation of the data such that Euclidean distances between points are preserved [12]. An Euclidean distance matrix \mathbf{D} is transformed by

$$\mathbf{B} = -\frac{1}{2} \mathbf{J}_N \mathbf{D}^{(2)} \mathbf{J}_N^T, \quad (2)$$

where $\mathbf{J}_N = \mathbf{I}_N - \frac{1}{N} \mathbf{1}_N \mathbf{1}_N^T$ is a centering matrix, \mathbf{I}_N is an $N \times N$ unity matrix, $\mathbf{D}^{(2)} = \mathbf{D} \circ \mathbf{D}$ is the entry-wise squared distance matrix, $\mathbf{1}_N$ is a $N \times 1$ vector of ones. \mathbf{B} is a positive semidefinite matrix with $\text{rank}(\mathbf{B}) = C$. Therefore \mathbf{B} has C positive eigenvalues, and $N - C$ eigenvalues equal to zero. The eigendecomposition of \mathbf{B} results in $\mathbf{B} = \mathbf{P} \mathbf{\Lambda} \mathbf{P}^T = \left(\mathbf{P} \mathbf{\Lambda}^{\frac{1}{2}} \right) \times \left(\mathbf{P} \mathbf{\Lambda}^{\frac{1}{2}} \right)^T = \mathbf{X} \mathbf{X}^T$, where $\mathbf{\Lambda} = \text{diag}(\lambda_1, \lambda_2, \dots, \lambda_C)$, and $\mathbf{\Lambda}^{\frac{1}{2}} = \text{diag}(\sqrt{\lambda_1}, \sqrt{\lambda_2}, \dots, \sqrt{\lambda_C})$, correspond to the nonzero eigenvalues of \mathbf{B} . Hence, the signals \mathbf{X} are composed of C components with N time points.

The distance matrix \mathbf{D} is required to be a valid distance matrix and to be conditionally negative definite in order to preserve the positive semidefiniteness of \mathbf{B} . $\mathbf{D} = [d_{ij}]$ based on the unweighted adjacency matrix $\mathbf{A} = [a_{ij}]$ has been defined as

$$d_{ij} = \begin{cases} 0, & i = j, \\ 1, & a_{i,j} = 1 \text{ and } i \neq j, \\ \gamma, & a_{i,j} = 0 \text{ and } i \neq j, \end{cases} \quad (3)$$

where γ is a parameter that ensures the conditional negative definiteness of \mathbf{D} . Here we consider $\gamma = 1 + \frac{1}{N}$, as in [13]. It is important to note that \mathbf{D} does not contain information about the distance between vertices, and only provides information related to whether the vertices are connected or not.

C. Phase Synchrony

In the construction of a weighted connectivity graph from EEG signals each vertex corresponds to an electrode and weights are obtained from the phase synchrony between two regions. Here, the signal's instantaneous phase is based on the RID-Rihaczek time-frequency distribution as proposed in [14]. For a signal x_i , define $C_i(t, \omega)$ to be its complex RID-Rihaczek time-frequency distribution, given by

$$C_i(t, \omega) = \int \int \underbrace{\exp\left(-\frac{(\theta\tau)^2}{\sigma}\right)}_{\text{Choi-Williams kernel}} \underbrace{\exp\left(j\frac{\theta\tau}{2}\right) A_i(\theta, \tau)}_{\text{Rihaczek kernel}} e^{-j(\theta t + \tau\omega)} d\tau d\theta, \quad (4)$$

where $A_i(\theta, \tau)$ is the ambiguity function of x_i :

$$A_i(\theta, \tau) = \int x_i\left(u + \frac{\tau}{2}\right) x_i^*\left(u - \frac{\tau}{2}\right) e^{j\theta u} du. \quad (5)$$

The time-varying phase of the signal x_i is computed as

$$\Phi_i(t, \omega) = \arg \left[\frac{C_i(t, \omega)}{|C_i(t, \omega)|} \right]. \quad (6)$$

Similarly, the phase difference between two signals x_i and x_j can be computed as

$$\Phi_{i,j}(t, \omega) = \arg \left[\frac{C_i(t, \omega)}{|C_i(t, \omega)|} \frac{C_j^*(t, \omega)}{|C_j(t, \omega)|} \right]. \quad (7)$$

The Phase Locking Value (PLV) between two signals x_i and x_j as a function of time and frequency [15] is defined by

$$PLV_{i,j}(t, \omega) = \left| \frac{1}{N} \sum_{k=1}^N \exp\left(j\Phi_{i,j}^k(t, \omega)\right) \right|, \quad (8)$$

where N corresponds to the total number of trials and $\Phi_{i,j}^k(t, \omega)$ is the phase difference between x_i and x_j as defined by (7) for the k^{th} trial.

III. RESISTANCE DISTANCE BASED NETWORK TO SIGNAL TRANSFORMATION

A. Resistance distance

In order to extend the CMDS based network to signal transform to weighted graphs, we consider the resistance distance matrix of a graph, denoted as \mathbf{R} . The resistance distance r_{ij} between vertices i and j is defined through the Moore-Penrose pseudo inverse of \mathbf{L} , \mathbf{L}^\dagger [5]

$$r_{ij} = (\mathbf{L}^\dagger)_{ii} + (\mathbf{L}^\dagger)_{jj} - 2(\mathbf{L}^\dagger)_{ij}. \quad (9)$$

Alternate definitions of \mathbf{R} also exist, based on the determinant of the Laplacian matrix [16]. It is also related to random walks, where the resistance distance between two vertices is proportional to the expected commute time of a random walk on the graph [17]. The resistance distance is a valid distance measure, satisfying the following properties [18]:

$$\begin{aligned} r_{i,j} &\geq 0 \text{ for all } i, j \text{ with equality if and only if } i = j, \\ r_{i,j} &= r_{j,i}, \\ r_{i,j} + r_{j,k} &\geq r_{i,k}. \end{aligned} \quad (10)$$

$\mathbf{R} = [r_{ij}]$ is a matrix of resistance distances, where each entry r_{ij} corresponds to the squared Euclidean distance [11]. In a connected graph, $r_{ij} \leq l_{ij}$, where l_{ij} is the shortest path distance, and equality holds when there is only one path between i and j [17]. Using \mathbf{R} , (2) is reformulated as

$$\mathbf{B} = -\frac{1}{2} \mathbf{J}_N \mathbf{R} \mathbf{J}_N^T, \quad (11)$$

to obtain a mapping to the Euclidean space and the signals \mathbf{X} are obtained as before (see (2)).

B. Reconstruction of the original graph

If the signals \mathbf{X} are not distorted, then in principle the resistance distance matrix \mathbf{R} can be recovered from the signals through the computation of the squared Euclidean distance between the points

$$\hat{\mathbf{R}}(X)_{ij} = \sum_{c=1}^C (x_{ic} - x_{jc})^2, \quad (12)$$

where C corresponds to the total number of components. It is possible to recover the original adjacency matrix from $\hat{\mathbf{R}}$, for both weighted and unweighted graphs as follows. First, we introduce τ [18] as

$$\tau_i = 2 - \sum_{j \neq i} \hat{r}(i, j). \quad (13)$$

For the next step, since \mathbf{R} is nonsingular [11], we consider the following expression of $\hat{\mathbf{R}}^{-1}$ which follows from the inverse of Euclidean distance matrices [19]:

$$\hat{\mathbf{R}}^{-1} = -\frac{1}{2}\hat{\mathbf{L}} + \frac{1}{\tau' \hat{\mathbf{R}} \tau} \tau \tau'. \quad (14)$$

From (14), the Laplacian matrix $\hat{\mathbf{L}}$ is estimated as

$$\hat{\mathbf{L}} = -2(\hat{\mathbf{R}}^{-1} - \frac{1}{\tau' \hat{\mathbf{R}} \tau} \tau \tau'). \quad (15)$$

Given an estimate of the Laplacian matrix, the degree matrix $\hat{\Delta}$ is estimated as the diagonal matrix whose elements are the diagonal entries of $\hat{\mathbf{L}}$

$$\hat{\Delta} = \text{diag}(\hat{L}_{1,1}, \hat{L}_{2,2}, \dots, \hat{L}_{N,N}). \quad (16)$$

Finally, the weighted adjacency matrix \hat{W} is found as

$$\hat{W} = \hat{\Delta} - \hat{\mathbf{L}}. \quad (17)$$

IV. RESULTS

In this section, we first compare the signals obtained from graphs based on the distance \mathbf{D} in (3) and the proposed resistance distance matrix \mathbf{R} for unweighted graphs. Next, we present signals obtained from weighted graphs as well as network reconstruction from these signals. Finally, we show how the proposed method can be applied to functional connectivity networks constructed from EEG to differentiate between the network structures obtained from two different experimental conditions.

A. Unweighted graphs

We first compare the signals obtained from binary ring lattice network using the original distance measure \mathbf{D} and the proposed resistance-based measure. For a ring lattice network consisting of 64 vertices, the proposed method results in sinusoidal signals, similar to the original method (Fig. 1), as expected from [5]. Based on the resistance distance, as the number of edges, K , increases, the amplitude of the signals decreases (Fig. 1 (a) and Fig. 1 (b)). Also, the amplitude of components decreases as the component number increases. In contrast, the original method does not capture the changes in the network's connectivity (Fig. 1 (c) and Fig. 1 (d)). It is known that the pairwise resistance r_{ij} decreases when edges are added or weights are increased [17]. Hence, as K increases the entries of the resistance distance matrix \mathbf{R} decreases. Therefore, the graph signal representation based on \mathbf{R} not only provides information about the type of network, but also yields information about its degree distribution.

B. Results from weighted graphs

The proposed method was also assessed on a weighted stochastic block model consisting of 150 vertices. Fig. 2 illustrates the signal representations (first 3 and 4 components) of networks for different connection probabilities (Fig. 2 (a) and Fig. 2 (b)) and for different number of blocks (Fig. 2 (c) and Fig. 2 (d)). It can be seen from these figures that the first $K - 1$ components directly correspond to

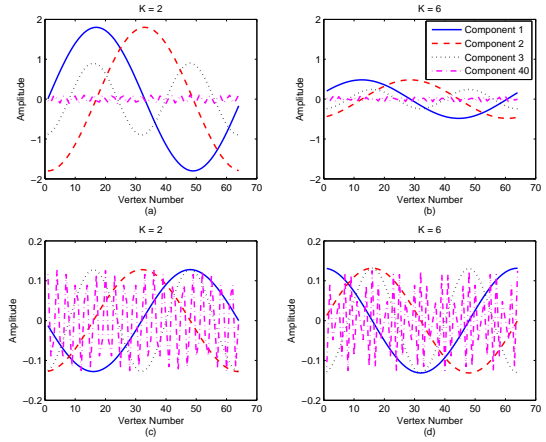


Fig. 1: Signal representation of ring lattice network. Top: Resistance distance; (a) $K = 2$; (b) $K = 6$. Bottom: Distance \mathbf{D} ; (c) $K = 2$; (d) $K = 6$.

individual clusters, with the K^{th} component being an impulse. Thus, the number of blocks in the network can be inferred by observing its components. In addition, the amplitude of the peak is inversely proportional to the connection probability.

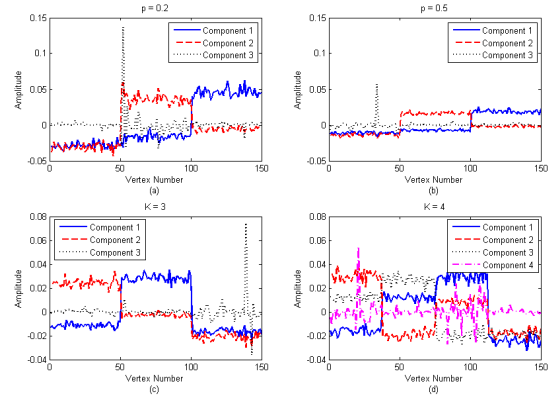


Fig. 2: Signals constructed from a weighted stochastic block network. Top: First three components corresponding to a network with $K = 3$ blocks, (a) $p = 0.2$; (b) $p = 0.5$. Bottom: (c) First three components corresponding to a network with $K = 3$ blocks, $p = 0.3$; (d) First three components corresponding to a network with $K = 4$ blocks, $p = 0.3$.

Fig. 3 shows the original and reconstructed adjacency matrices for a stochastic block network with 3 blocks, $p = 0.3$, and a small-world network, with probability of connection $p = 0.5$ and $k = 6$ nearest neighbors. Clearly, the proposed method is accurate in the reconstruction of both the structure and weights of the network. For 50 simulations, we computed the reconstruction error based on the Frobenius norm of the difference between the reconstructed and original adjacency matrices, $\frac{1}{N(N-1)} \|\mathbf{A} - \hat{\mathbf{A}}\|_F$. Table I shows the reconstruction errors for both networks.

C. EEG Data from a Cognitive Control Study

The proposed measure was evaluated on an EEG data set from a cognitive control-related error processing study. We studied the

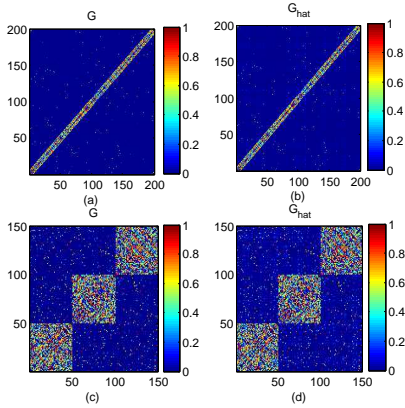


Fig. 3: Original and reconstructed adjacency matrices. Top: Small-world network, (a) Original; (b) Reconstructed. Bottom: Stochastic block network, (c) Original; (d) Reconstructed.

TABLE I: Reconstruction errors

Network	Error (mean \pm st.dev.)
Small-World	$9.17 \times 10^{-5} \pm 4.48 \times 10^{-6}$
Stochastic Block	$1.7 \times 10^{-3} \pm 2.09 \times 10^{-5}$

error-related negativity (ERN), an event potential which reaches its maximum amplitude within 100 ms after errors are made in simple reaction time tasks [20]. This potential has been related to increased synchronization among the central and frontal regions in the theta band (4–8 Hz) [21], when compared to central and parietal regions [22]. EEG data was provided from a previously published study where subjects performed a speeded-response flanker task [23]. In this experiment subjects were required to correctly identify the target letter, located at the center of a five-letter string. EEG activity from error and correct responses was recorded and all epochs were processed offline for removal of eye movement artifacts and volume conduction correction using the Current Source Density (CSD) Toolbox [24]. A total of nineteen subjects with error trials ranging from 20 to 61 (36.78 ± 13.72 , mean \pm st.dev.), were considered in this analysis and the same number of correct responses was chosen randomly.

In order to construct functional connectivity networks, phase synchrony between pairs of electrodes is computed for both error and correct responses. A network for each subject was constructed by averaging the PLV over the frequency bins corresponding to the theta band, 4-8 Hz, and the ERN interval, 25–75 ms. A final network for error and correct responses was obtained by averaging over subjects. The optimal ordering of the nodes was obtained from the Cuthill-McKee algorithm. These networks were transformed into signals by using (11). The magnitude of the Fourier transform of each component for error and correct responses are shown in Fig. 4 (a) and Fig. 4 (b), respectively. The spectrum of error responses contain high energy for low frequencies in the first few components, and as the component number increases this energy shifts until it reaches the higher frequencies for the last components. On the other hand, there is no clear trend in the spectrum corresponding to correct responses.

From this spectral information, it is possible to correlate the error and correct responses to well-known network structures. For both error and correct responses, we computed the spectral centroid for each component and examined its correlation with that of a small

world network for different number of nearest neighbors K and probability of rewiring p . Fig. 5 shows error bars obtained after 50 simulations of the small world network. Error responses are highly correlated with a small world network, and this correlation is inversely proportional to the number of nearest neighbors. On the other hand, correct responses are less correlated, but still show some small-world behavior for small number of neighbors. This is in line with previously published work, where we showed increased small-world characteristics for ERN compared to correct-related negativity (CRN) [25]. Thus, this approach provides an alternative method to characterize the network’s behavior for each cognitive condition.

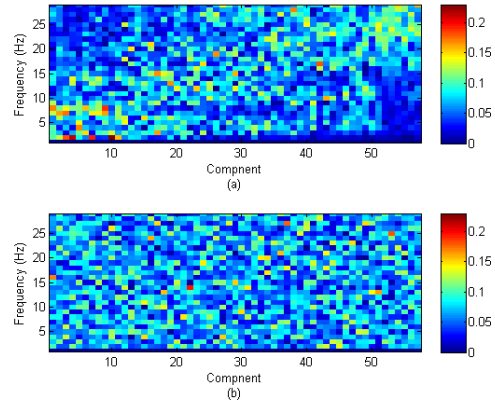


Fig. 4: Fourier transform for each component. (a) Error responses; (b) Correct responses.

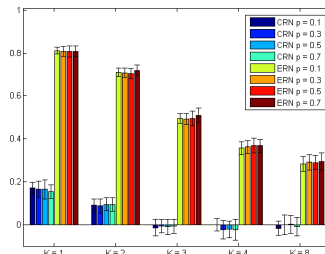


Fig. 5: Correlations between the spectral centroid of cortical responses and small world network model.

V. CONCLUSION AND FUTURE WORK

In this paper, a new network to signal transformation based on the resistance distance has been proposed for weighted networks. The proposed method reveals structural attributes of the graphs, not perceivable by previously proposed distance matrices. Furthermore, the proposed method can characterize the behavior of functional connectivity networks under different cognitive conditions. Future work will focus on the processing of the network signals for applications such as graph filtering and extensions to temporal networks.

ACKNOWLEDGMENT

The authors would like to thank Dr. Jason Moser from the Psychology Department at Michigan State University for providing the EEG data.

REFERENCES

- [1] D. Papo, M. Zanin, J. A. Pineda-Pardo, S. Boccaletti, and J. M. Buldú, "Functional brain networks: great expectations, hard times and the big leap forward," *Philosophical Transactions of the Royal Society of London B: Biological Sciences*, vol. 369, no. 1653, p. 20130525, 2014.
- [2] K. J. Friston, "Functional and effective connectivity: a review," *Brain connectivity*, vol. 1, no. 1, pp. 13–36, 2011.
- [3] M. E. Bolanos and S. Aviyente, "Quantifying the functional importance of neuronal assemblies in the brain using laplacian hückel graph energy," in *Acoustics, Speech and Signal Processing (ICASSP), 2011 IEEE International Conference on*. IEEE, 2011, pp. 753–756.
- [4] D. Shuman, S. K. Narang, P. Frossard, A. Ortega, P. Vandergheynst *et al.*, "The emerging field of signal processing on graphs: Extending high-dimensional data analysis to networks and other irregular domains," *Signal Processing Magazine, IEEE*, vol. 30, no. 3, pp. 83–98, 2013.
- [5] Y. Shimada, T. Ikeguchi, and T. Shigehara, "From networks to time series," *Physical review letters*, vol. 109, no. 15, p. 158701, 2012.
- [6] Y. Haraguchi, Y. Shimada, T. Ikeguchi, and K. Aihara, "Transformation from complex networks to time series using classical multidimensional scaling," in *Artificial Neural Networks–ICANN 2009*. Springer, 2009, pp. 325–334.
- [7] T. Weng, Y. Zhao, M. Small, and D. D. Huang, "Time-series analysis of networks: Exploring the structure with random walks," *Physical Review E*, vol. 90, no. 2, p. 022804, 2014.
- [8] X. Li, X. Liu, and C. K. Tse, "Recent advances in bridging time series and complex networks," in *Circuits and Systems (ISCAS), 2013 IEEE International Symposium on*. IEEE, 2013, pp. 2505–2508.
- [9] R. Hamon, P. Borgnat, P. Flandrin, and C. Robardet, "Nonnegative matrix factorization to find features in temporal networks," in *Acoustics, Speech and Signal Processing (ICASSP), 2014 IEEE International Conference on*. IEEE, 2014, pp. 1065–1069.
- [10] D. J. Klein and M. Randić, "Resistance distance," *Journal of Mathematical Chemistry*, vol. 12, no. 1, pp. 81–95, 1993.
- [11] R. Bapat, "Resistance matrix of a weighted graph," *Communications in Mathematical and in Computer Chemistry/MATCH*, vol. 50, pp. 73–82, 2004.
- [12] F. Rossi, "Visualization methods for metric studies," in *Proceedings of the International Workshop on Webometrics, Informetrics and Scientometrics*, 2006, pp. 356–366.
- [13] R. Hamon, P. Borgnat, P. Flandrin, and C. Robardet, "From graphs to signals and back: Identification of network structures using spectral analysis," 2015.
- [14] S. Aviyente and A. Mutlu, "A time-frequency-based approach to phase and phase synchrony estimation," *IEEE Transactions on Signal Processing*, vol. 59, no. 7, pp. 3086–3098, 2011.
- [15] J.-P. Lachaux, E. Rodriguez, J. Martinerie, F. J. Varela *et al.*, "Measuring phase synchrony in brain signals," *Human brain mapping*, vol. 8, no. 4, pp. 194–208, 1999.
- [16] R. B. Bapat, I. Gutmana, and W. Xiao, "A simple method for computing resistance distance," *Zeitschrift für Naturforschung A*, vol. 58, no. 9–10, pp. 494–498, 2003.
- [17] W. Ellens, F. Spieksma, P. Van Mieghem, A. Jamakovic, and R. Kooij, "Effective graph resistance," *Linear algebra and its applications*, vol. 435, no. 10, pp. 2491–2506, 2011.
- [18] R. B. Bapat, *Graphs and matrices*. Springer, 2010.
- [19] R. Balaji and R. Bapat, "On euclidean distance matrices," *Linear algebra and its applications*, vol. 424, no. 1, pp. 108–117, 2007.
- [20] J. S. Moser, T. P. Moran, H. S. Schroder, M. B. Donnellan, and N. Yeung, "On the relationship between anxiety and error monitoring: a meta-analysis and conceptual framework," *Frontiers in human neuroscience*, vol. 7, 2013.
- [21] J. Cavanagh, M. Cohen, and J. Allen, "Prelude to and resolution of an error: EEG phase synchrony reveals cognitive control dynamics during action monitoring," *The Journal of Neuroscience*, vol. 29, no. 1, pp. 98–105, 2009.
- [22] M. Cohen, "Error-related medial frontal theta activity predicts cingulate-related structural connectivity," *Neuroimage*, vol. 55, no. 3, pp. 1373–1383, 2011.
- [23] T. P. Moran, E. M. Bernat, S. Aviyente, H. S. Schroder, and J. S. Moser, "Sending mixed signals: Worry is associated with enhanced initial error processing but reduced call for subsequent cognitive control," *Social cognitive and affective neuroscience*, p. nsv046, 2015.
- [24] J. Kayser and C. E. Tenke, "Principal components analysis of laplacian waveforms as a generic method for identifying erp generator patterns: I. evaluation with auditory oddball tasks," *Clinical neurophysiology*, vol. 117, no. 2, pp. 348–368, 2006.
- [25] M. Bolanos, E. M. Bernat, B. He, and S. Aviyente, "A weighted small world network measure for assessing functional connectivity," *Journal of neuroscience methods*, vol. 212, no. 1, pp. 133–142, 2013.